Supporting Information

Ferromagnetic Archimedean Polyhedra $\{Fe_{24}M_{18}\}$ (M = Fe, Ni, and Mn) with Tunable Electron Configurations

Wen Wen,[a] Yin-Shan Meng,*[a] Cheng-Qi Jiao,[a] Qiang Liu,[a] Hai-Lang Zhu,[a] Ya-Ming Li,[a] Hiroki Oshio[a] and Tao Liu*[a]

[a]State Key Laboratory of Fine Chemicals, Dalian University of Technology, Dalian, 116024, China.

*Corresponding author. Email: mengys@dlut.edu.cn (Y.-S. Meng); liutao@dlut.edu.cn (T. Liu)

Contents

Experimental Section

Materials

All chemical reagents were acquired from commercial sources and used without further purification. $[Bu_4N][Fe(Tp)(CN)_3]$ (Tp = hydrotris(pyrazolyl)borate) was synthesized according to the literature's method.[S1]

Synthesis of compounds 1-3

Compounds **1-3** were constructed through the reaction of $[Bu_4N][Fe^{III}(Tp)(CN)_3]$, pyridine-4-carboxaldehyde and $M(ClO_4)_2{\cdot}6H_2O$ (M = Fe^{2+}/Ni^{2+}/Mn^{2+}). 1.0 mL aqueous solution of $M(ClO_4)_2{\cdot}6H_2O$ (0.010 mmol) was placed at the bottom of a test tube, a mixture of methanol and water (1: 1, v/v, 6 mL) was gently layered on the top of the solution, and then 1.0 mL methanol solution of $Bu_4N[Fe^{III}(Tp)(CN)_3]$ (0.010 mmol) and pyridine-4-carboxaldehyde (0.020 mmol) was carefully added as the third layer. After a few weeks, cubic crystals of **1-3** were collected. Yield for compound **1**: 38% based on $Fe(ClO_4)_2{\cdot}6H_2O$. Anal. Calcd (%) for $C_{360}H_{354}B_{24}Fe_{42}N_{228}O_{54}$: C 38.12, H 3.15, N 28.15; Found: C 37.98, H 3.19, N 28.10. Yield for compound **2**: 29% based on $Ni(ClO_4)_2{\cdot}6H_2O$. Anal. Calcd (%) for $C_{360}H_{350}B_{24}Fe_{24}Ni_{18}N_{228}O_{50}$: C 38.17, H 3.11, N 28.20; Found: C 37.84, H 3.23, N 27.90. Yield for compound **3**: 27% based on $Mn(ClO_4)_2{\cdot}6H_2O$. Anal. Calcd (%) for $C_{360}H_{353}B_{24}Fe_{32}Mn_{10}N_{228}O_{52}$: C 38.26, H 3.15, N 28.26; Found: C 37.87, H 3.19, N 27.92.

Structure determination and refinement

The single-crystal XRD data for **1-3** were collected on Bruker D8 Venture CMOS-based diffractometer (Mo-Kα radiation, λ = 0.71073 Å) using the SMART and SAINT programs. Final unit cell parameters were based on all observed reflections from integration of all frame data. The structures were solved with the ShelXT structure solution program using Intrinsic Phasing and refined with the ShelXL refinement package using Least Squares minimization that implanted in Olex2. For all compounds, all non-hydrogen atoms were refined anisotropically and the hydrogen atoms of organic ligands were located geometrically and fixed isotropic thermal parameters. Due to the strong disordering of the H_2O molecular, some hydrogen atoms could not be added. For **3-Mn**, a part of the $[Fe^{III}(Tp)(CN)_3]^-$ unit decomposed to release Fe^{III} ions into the $[Fe(NC)_4(H_2O)_2]$ and $[Fe(NC)_4(L)(H_2O)]$ moieties. The exact molecular formula and molecular weight were calculated from the real structure and unmatched with the refinement results.

IR Spectra measurements.

Infrared spectra were measured on KBr pellets samples using a Nicolet iS10 FT-IR spectrometer.

XPS Spectra measurements.

XPS spectra were measured using ESCALAB XI+ from thermo company and simulated in XPSPEAK41.

^{57}Fe Mössbauer spectra measurement

Zero-field ^{57}Fe Mössbauer spectra were recorded on a WSS-10 spectrometer with a proportional counter. The temperature of the sample was controlled by Model 22C digital temperature controller from Janis Research Company. The Doppler velocity of the spectrometer was calibrated with respect to α-Fe.

Magnetic Studies

Magnetic measurements of samples were performed on a Quantum Design PPMS-9. Measurements were performed using finely ground microcrystalline powders restrained by the parafilm with polycarbonate capsules. Data were corrected for the diamagnetic contribution calculated from Pascal constants and background from the parafilm and capsules.

References

S1 R. Lescouëzec, J. Vaissermann, F. Lloret, M. Julve and M. Verdaguer, Ferromagnetic Coupling between Low- and High-Spin Iron(III) Ions in the Tetranuclear Complex fac-$\{[Fe^{III}\{HB(pz)_3\}(CN)_2(\mu\text{-}CN)]_3Fe^{III}(H_2O)_3\}\cdot 6H_2O$ ($[HB(pz)_3]^-$ = Hydrotris(1-pyrazolyl)borate), *Inorg. Chem.*, 2002, **41**, 5943-5945.

Table S1. Crystal Data and Structure Refinements for compounds **1-3** at 150 K.

	1-Fe	**2-Ni**	**3-Mn**
CCDC	2068740	2068741	2068760
Formula	$C_{360}H_{354}B_{24}Fe_{42}N_{228}O_{54}$	$C_{360}H_{350}B_{24}Fe_{24}Ni_{18}N_{228}O_{50}$	$C_{360}H_{353}B_{24}Fe_{32}Mn_{10}N_{228}O_{52}$
Fw	11343.12	11326.36	11301.04
Crystal system	Cubic	Cubic	Cubic
Space group	$Pn\bar{3}n$	$Pn\bar{3}n$	$Pn\bar{3}n$
a (Å)	30.7285(8)	30.7270(3)	30.9319(9)
b (Å)	30.7285(8)	30.7270(3)	30.9319(9)
c (Å)	30.7285(8)	30.7270(3)	30.9319(9)
α (°)	90	90	90
β (°)	90	90	90
γ (°)	90	90	90
V (Å^3)	29015(2)	29010.9(8)	29595(3)
Z	2	2	2
D_{calc} (g/cm^3)	1.292	1.291	1.260
F (000)	11400.0	11408.0	11308.0
Reflections collected	89025	75511	141076
Unique reflections (R_{int})	0.0682	0.0856	0.0720
Goodness–of–fit on F^2	1.019	1.025	1.055
R_1 [I>2$\sigma(I)$][a]	0.0622	0.0553	0.0569
wR_2 [I>2$\sigma(I)$][b]	0.1700	0.1684	0.1626

$R_1 = \Sigma (|F_0|-|F_C|) / \Sigma |F_0|$; $wR_2 = [\Sigma w (|F_0|-|F_C|)^2 / \Sigma w F_0^2]^{1/2}$.

Table S2. Selected Bond Lengths (Å) and Bond Angles (˚) for compound **1**.

Compound 1^{150K}			
Bond length (Å)			
Fe1–O1	2.029(4)	Fe2–N7^{4}	2.022(3)
Fe1–N8^{1}	2.072(2)	Fe2–N7^{5}	2.022(3)
Fe1–N8^{2}	2.072(2)	Fe2–N7	2.022(3)
Fe1–N9	2.044(3)	Fe3–N2	1.999(2)
Fe1–N9^{3}	2.044(3)	Fe3–N4	2.000(2)
Fe1–N10	2.197(3)	Fe3–N6	2.013(3)
Fe2–O2	2.124(9)	Fe3–C10	1.853(3)
Fe2–O3	2.098(7)	Fe3–C11	1.886(3)
Fe2–N7	2.022(3)	Fe3–C12	1.880(3)
Bond angle (°)			
O1–Fe1–N8^{1}	92.29(7)	N7–Fe2–O3	88.51(11)
O1–Fe1–N8^{2}	92.29(7)	N7^{4}–Fe2–N7^{1}	89.961(6)
O1–Fe1–N9^{3}	90.31(8)	N7^{1}–Fe2–N7^{5}	177.0(2)
O1–Fe1–N9	90.30(8)	N7^{4}–Fe2–N7^{5}	89.961(6)
O1–Fe1–N10	180.00(3)	N7–Fe2–N7^{4}	177.0(2)
N8^{1}–Fe1–N8^{2}	175.43(15)	N7–Fe2–N7^{1}	89.960(6)
N8^{2}–Fe1–N10	87.71(7)	N7–Fe2–N7^{5}	89.962(6)
N8^{1}–Fe1–N10	87.71(7)	N2–Fe3–N4	87.40(10)
N9–Fe1–N8^{1}	89.79(10)	N2–Fe3–N6	87.67(10)
N9–Fe1–N8^{2}	90.18(10)	N4–Fe3–N6	86.63(10)
N9^{3}–Fe1–N8^{1}	90.18(10)	C10–Fe3–N2	93.89(12)
N9^{3}–Fe1–N8^{2}	89.79(10)	C10–Fe3–N4	173.88(12)
N9^{3}–Fe1–N9	179.39(16)	C10–Fe3–N6	87.44(12)
N9^{3}–Fe1–N10	89.69(8)	C10–Fe3–C11	88.53(13)
N9–Fe1–N10	89.70(8)	C10–Fe3–C12	90.73(13)
O3–Fe2–O2	180.0	C11–Fe3–N2	89.41(11)
N7^{1}–Fe2–O2	91.49(11)	C11–Fe3–N4	97.47(11)
N7^{4}–Fe2–O2	91.49(11)	C11–Fe3–N6	174.85(12)
N7^{5}–Fe2–O2	91.49(11)	C12–Fe3–N2	175.21(11)
N7–Fe2–O2	91.49(11)	C12–Fe3–N4	87.87(11)
N7^{5}–Fe2–O3	88.51(11)	C12–Fe3–N6	91.28(12)
N7^{4}–Fe2–O3	88.51(11)	C12–Fe3–C11	91.97(13)
N7^{1}–Fe2–O3	88.51(11)		

^{1}+X,+Z,3/2-Y;^{2}1/2-Z,1/2-X,+Y;^{3}1/2-Y,1/2-X,3/2-Z;^{4}+X,3/2-Y,3/2-Z;^{5}+X,3/2-Z,+Y;^{6}1/2-Y,+Z,1/2-X

Table S3. Selected Bond Lengths (Å) and Bond Angles (°) for compound **2**.

Compound 2^{150K}			
Bond length (Å)			
Ni1–O1	2.064(9)	Ni2–N9	2.044(3)
Ni1–O2	2.090(9)	Ni2–$N9^{5}$	2.044(3)
Ni1–$N7^{1}$	2.024(3)	Ni2–N10	2.200(5)
Ni1–$N7^{2}$	2.024(3)	Fe1–N2	2.001(3)
Ni1–$N7^{3}$	2.024(3)	Fe1–N4	2.001(3)
Ni1–N7	2.024(3)	Fe1–N6	2.016(3)
Ni2–O3	2.018(5)	Fe1–C10	1.852(4)
Ni2–$N8^{4}$	2.070(3)	Fe1–C11	1.882(4)
Ni2–$N8^{1}$	2.070(3)	Fe1–C12	1.866(4)
Bond angle (°)			
O1–Ni1–O2	180.0	$N9^{5}$–Ni2–$N8^{4}$	89.63(12)
$N7^{1}$–Ni1–O1	91.46(13)	$N9^{5}$–Ni2–$N8^{1}$	90.33(12)
$N7^{2}$–Ni1–O1	91.46(13)	N9–Ni2–$N8^{1}$	89.62(12)
$N7^{3}$–Ni1–O1	91.46(13)	N9–Ni2–$N8^{4}$	90.33(12)
N7–Ni1–O1	91.45(13)	$N9^{5}$–Ni2–N9	179.0(2)
$N7^{1}$–Ni1–O2	88.54(13)	N9–Ni2–N10	89.48(10)
N7–Ni1–O2	88.55(13)	$N9^{5}$–Ni2–N10	89.48(10)
$N7^{2}$–Ni1–O2	88.54(13)	N2–Fe1–N4	87.44(12)
$N7^{3}$–Ni1–O2	88.54(13)	N2–Fe1–N6	87.47(13)
$N7^{1}$–Ni1–$N7^{2}$	89.963(7)	N4–Fe1–N6	86.81(13)
$N7^{3}$–Ni1–$N7^{2}$	89.963(7)	C10–Fe1–N2	94.10(15)
$N7^{3}$–Ni1–N7	89.960(7)	C10–Fe1–N4	174.07(15)
$N7^{2}$–Ni1–N7	177.1(3)	C10–Fe1–N6	87.54(15)
$N7^{1}$–Ni1–N7	89.966(7)	C10–Fe1–C11	88.27(16)
$N7^{3}$–Ni1–$N7^{1}$	177.1(3)	C10–Fe1–C12	90.67(16)
O3–Ni2–$N8^{4}$	92.62(9)	C11–Fe1–N2	89.58(14)
O3–Ni2–$N8^{1}$	92.62(9)	C11–Fe1–N4	97.47(14)
O3–Ni2–$N9^{5}$	90.52(10)	C11–Fe1–N6	174.69(15)
O3–Ni2–N9	90.52(10)	C12–Fe1–N2	175.04(14)
O3–Ni2–N10	180.00(18)	C12–Fe1–N4	87.68(14)
$N8^{1}$–Ni2–$N8^{4}$	174.75(19)	C12–Fe1–C6	91.37(15)
$N8^{1}$–Ni2–N10	87.38(9)	C12–Fe1–C11	91.94(16)
$N8^{4}$–Ni2–N10	87.38(9)		

^{1}+X,+Z,1/2-Y;^{2}+X,1/2-Z,+Y;^{3}+X,1/2-Y,1/2-Z;^{4}+Y,1/2-Z,1/2-X;^{5}1/2-Z,1/2-Y,1/2-X

Table S4. Selected Bond Lengths (Å) and Bond Angles (°) for compound **3**.

Compound 3^{150K}			
Bond length (Å)			
Fe1–N2	1.995(3)	Mn1–N7	2.118(3)
Fe1–N4	1.991(3)	Mn1–N7^{3}	2.118(3)
Fe1–N6	2.004(3)	Mn1–O1	2.118(5)
Fe1–C12	1.867(4)	Mn2–N9^{4}	2.073(3)
Fe1–C11	1.889(4)	Mn2–N9^{2}	2.073(3)
Fe1–C10	1.882(4)	Mn2–N9^{5}	2.073(3)
Mn1–N10	2.261(4)	Mn2–N9	2.073(3)
Mn1–N8^{1}	2.157(3)	Mn2–O2	2.200(10)
Mn1–N8^{2}	2.157(3)	Mn2–O3	2.131(11)
Bond angle (°)			
N2–Fe1–N6	86.74(11)	N7^{3}–Mn1–N8^{2}	89.57(11)
N4–Fe1–N2	87.70(11)	N7^{3}–Mn1–N7	179.8(2)
N4–Fe1–N6	88.12(12)	N7–Mn1–O1	89.88(9)
C12–Fe1–N2	174.52(14)	N7^{3}–Mn1–O1	89.88(9)
C12–Fe1–N4	93.83(14)	O1–Mn1–N10	180.0(3)
C12–Fe1–N6	88.05(14)	O1–Mn1–N8^{1}	92.25(9)
C12–Fe1–C11	88.49(15)	O1–Mn1–N8^{2}	92.25(9)
C12–Fe1–C10	89.75(15)	N9^{1}–Mn2–N9^{4}	174.8(3)
C11–Fe1–N2	96.78(13)	N9^{5}–Mn2–N9	174.8(3)
C11–Fe1–N4	90.11(13)	N9^{1}–Mn2–N9^{5}	89.883(12)
C11–Fe1–N6	175.99(13)	N9^{4}–Mn2–N9	89.884(12)
C10–Fe1–N2	88.71(13)	N9^{1}–Mn2–N9	89.881(12)
C10–Fe1–N4	176.41(13)	N9^{4}–Mn2–N9^{5}	89.883(12)
C10–Fe1–N6	91.73(14)	N9–Mn2–O2	87.41(13)
C10–Fe1–C11	90.26(15)	N9^{4}–Mn2–O2	87.41(13)
N8^{1}–Mn1–N10	87.75(9)	N9^{1}–Mn2–O2	87.41(13)
N8^{2}–Mn1–N10	87.75(9)	N9^{5}–Mn2–O2	87.41(13)
N8^{1}–Mn1–N8^{2}	175.50(17)	N9–Mn2–O3	92.59(13)
N7^{3}–Mn1–N10	90.12(9)	N9^{5}–Mn2–O3	92.59(13)
N7–Mn1–N10	90.12(9)	N9^{1}–Mn2–O3	92.59(13)
N7–Mn1–N8^{2}	90.44(11)	N9^{4}–Mn2–O3	92.59(13)
N7^{3}–Mn1–N8^{1}	90.44(11)	O3–Mn2–O2	180.0
N7–Mn1–N8^{1}	89.57(11)		

^{1}+Z,+Y,1/2-X;^{2}1/2-Z,+X,1/2-Y;^{3}1/2-X,1/2-Z,1/2-Y;^{4}1/2-Z,+Y,+X;^{5}1/2-X,+Y,1/2-Z;^{6}+Y,1/2-Z,1/2-X

Table S5. The Fe···Fe edge lengths for the squares, rectangles, and regular triangles for **1-3**.

	Squares (Å)	Rectangles (Å)	Regular triangles (Å)
1-Fe	6.775	6.775*7.306	7.306
2-Ni	6.778	6.778*7.304	7.304
3-Mn	6.847	6.847*7.392	7.392

Table S6. Mössbauer parameters for compounds **1-3** at 80 K.

	δ mm s^{-1}	ΔE_Q mm s^{-1}	Content %	Calcd. %	Assignments
1-Fe	0.05	0.49	56.07	57.14	$^{Tp}Fe^{II}_{LS}$
$[^{Tp}Fe^{II}_{LS}]_{24}[Fe^{III}_{HS}]_{18}$	0.45	0.87	43.93	42.86	Fe^{III}_{HS}
2-Ni	0.17	0.47	40.26	41.67	$^{Tp}Fe^{II}_{LS}$
$[^{Tp}Fe^{III}_{LS}]_{14}[^{Tp}Fe^{II}_{LS}]_{10}[Ni^{II}]_{18}$	0.03	1.05	59.74	58.33	$^{Tp}Fe^{III}_{LS}$
3-Mn	0.04	0.49	52.59	53.13	$^{Tp}Fe^{II}_{LS}$
$[^{Tp}Fe^{III}_{LS}]_{7}[^{Tp}Fe^{II}_{LS}]_{17}[Fe^{III}_{HS}]_{8}[Mn^{II}]_{10}$	-0.06	1.07	22.58	21.88	$^{Tp}Fe^{III}_{LS}$
	0.43	0.90	24.83	25.00	Fe^{III}_{HS}

Table S7. ICP-AES experiments results for compounds **1-3**.

	Element	Concentration (mg/L)	Concentration (mmol/L)	Elemental ratio
1-Fe	Fe	35.02	0.63	1.00
2-Ni	Fe	29.84	0.53	0.57
	Ni	23.34	0.40	0.43
3-Mn	Fe	34.20	0.61	0.75
	Mn	11.30	0.20	0.25

Table S8. The $\chi_m T$ value at 300 K and Curie-Weiss fitting value of **1-3**.

	1-Fe	**2-Ni**	**3-Mn**
$\chi_m T$-experimental ($cm^3 mol^{-1} K$)	75.82	31.84	80.40
$\chi_m T$-calculated ($cm^3 mol^{-1} K$)	78.75	32.68	83.19
Curie constant ($cm^3 mol^{-1} K$)	74.76	30.84	79.30
Weiss temperature (K)	3.24	4.22	3.28

Table S9. The ground spin state, ΔS_{max}–experimental and ΔS_{max}–calculated for **1-3**.

	1-Fe	**2-Ni**	**3-Mn**
S (ground spin state)	90/2	50/2	97/2
ΔS_{max}–experimental ($J\ kg^{-1}\ K^{-1}$)	17.48	9.46	19.84
ΔS_{max}–calculated ($J\ kg^{-1}\ K^{-1}$)	23.64	14.51	27.30

ΔS_{max}–calculated = $\Sigma R\ln(2s+1)$; $R = 8.314*10^3$ / M $J\ kg^{-1}\ K^{-1}$ (M represents formula weight)

Table S10. Summary of ΔS_{max} data based on ΔH at given temperature for discrete 3d-metal clusters.

Compounds	ΔS_{max} (J kg^{-1} K^{-1})	ΔH (T)	T_{max} (K)
$[Mn^{III}_8Mn^{IV}_4O_{12}(OAc)_{16}(H_2O)_4]\cdot 2HOAc\cdot 4H_2O$[49]	frequency-dependent MCE	3	1.8
$[Mn^{III}_8Mn^{IV}_4O_{12}(2\text{-}ClPhCO_2)_{16}(H_2O)_4]$ $CH_2Cl_2\cdot 5H_2O$[50]	4.3	3	2.5
$[Fe^{III}_8(\mu3\text{-}O)_2(\mu2\text{-}OH)_{12}(tacn)_6]Br_8\cdot 9H_2O$[51]	frequency-dependent and anisotropic MCE	3	1.7
$[Fe^{III}_{14}O_6(bta)_6(OMe)_{18}Cl_6]$[52]	17.6	7	6.0
$[Fe^{III}_{14}O_6(ta)_6(OMe)_{18}Cl_6]$[53]	20.3	7	6.0
$[Mn^{III}_6Mn^{II}_4O_4Br_4(amp)_6(H_2amp)_3(H_3amp)]$ $Br_{38}(C_6H_{14})$[54]	13.0	7	2.2
$[Mn^{III}_6Mn^{II}_4(OH)_6I_4(amp)_4(Hamp)_4(EtOH)_4]$ $I_4\cdot 12(EtOH)$[55]	17.0	7	5.2
$[Mn^{III}_6Mn^{II}_8(OH)_2I_4(Hpeol)_4(H_2peol)_6(EtOH)_6]I_4$[56]	25.0	7	3.8
$[Mn^{II}(bpy)_3]_{1.5}[Mn^{IV}_8Mn^{II}_{24}(thme)_{16}(bpy)_{24}$ $(N_3)_{12}(OAc)_{12}](ClO_4)_{11}$[56]	18.2	7	1.6
$[Mn^{III}_6Mn^{II}_4(\mu_3\text{-}O)_4(Hmpt)_6(\mu_3\text{-}N_3)_3(\mu_3\text{-}Br)(Br)]$ $(N_3)_{0.7/}(Br)_{0.33}MeCN\cdot 2MeOH$[57]	10.3	9	2.6
$[Mn^{III}_{11}Mn^{II}_6(\mu_4\text{-}O)_8(\mu_3\text{-}Cl)_4(\mu,\mu_3\text{-}OAc)_2(\mu,\mu\text{-}$ $dmp)_{10}Cl_{2.34}(OAC)_{0.66}(py)_3(MeCN)_2]\cdot 7MeCN$[58]	13.3	9	5.2
$[Mn^{III}_{12}Mn^{II}_7(\mu_4\text{-}O)_8(Hhmmp)_{12}(\mu_3\text{-}\eta^1N_3)_8$ $(MeCN)_6]Cl_2\cdot MeCN\cdot 10MeOH$[58]	8.9	7	4.2
$[Mn^{III}_{12}Mn^{II}_7O_8(Hhmph)_{12}(N_3)_3(MeO)_{5.5}$ $(MeOH)_{3.5}(H_2O)_{1.5}(OH)_{0.5}](OAc)\cdot 10H_2O$[58]	9.0	7	7.0
$[Na_2Mn^{III}_{11}Mn^{II}_4O_8(Hhmph)_{10}(OAc)_2(H_2O)_2$ $(MeO)_{1.5}(N_3)_{2.5}](OAc)\cdot 10H_2O\cdot 2MeOH$[59]	9.5	7	6.0
$Mn^{II}_4(N_3)_{7.3}Cl_{0.7}(dafo)_4$[59]	19.34	5	4.0
$[Fe^{III}_{17}O_{16}(OH)_{12}(py)_{12}Br_4]Br_3$[60]	8.9	7	2.7
$[Mn^{III}_{36}Mn^{II}_{13}(\mu_4\text{-}O)_{32}(\mu_3\text{-}OCH_3)_8(\mu_3\text{-}hp)_{24}(O_2CH)_6$ $(DMF)_{12}](OH)_8$[61]	6.4	7	10
$[Mn^{III}_{20}Mn^{II}_5Na_4(\mu_4\text{-}O)_{16}(\mu_3\text{-}OCH_3)_4(\mu_3\text{-}hp)_{16}$ $(O_2CCH_3)_4(O_2CH)(DMF)_8]\cdot(O_2CH)$[61]	7.7	7	8

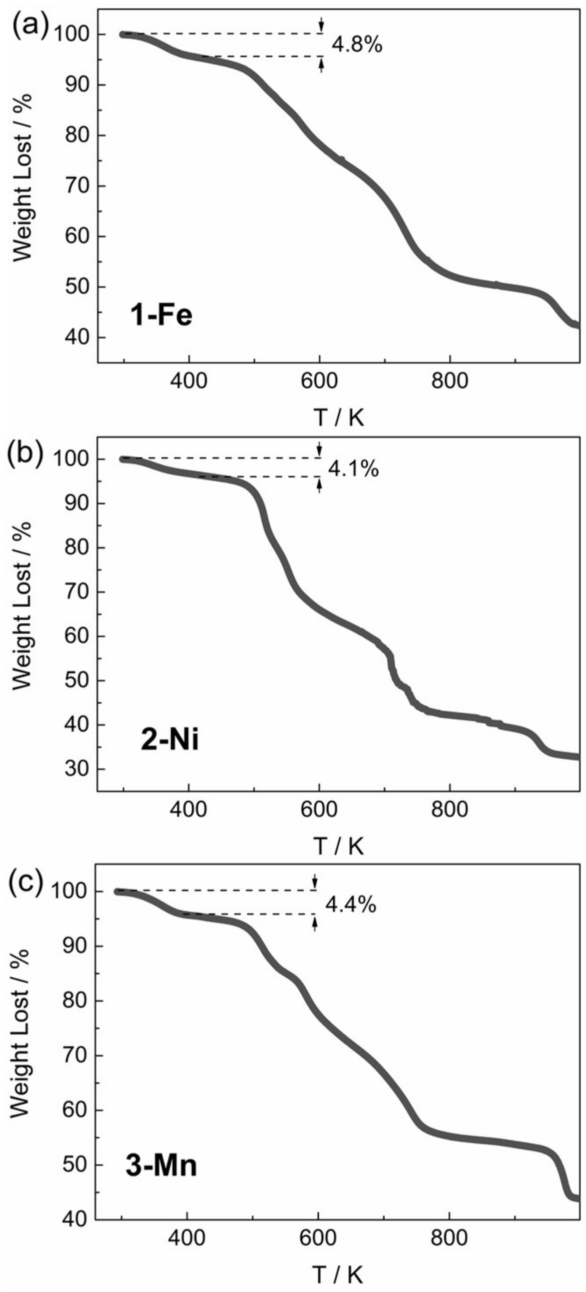

Fig. S1. Thermo-gravimetric analysis curve for compounds **1-3** in the Nitrogen atmosphere with the sweeping rate of 10 K min^{-1}. The weight lost were all attribute to H_2O molecules that better accord with the molecular formula of each compounds.

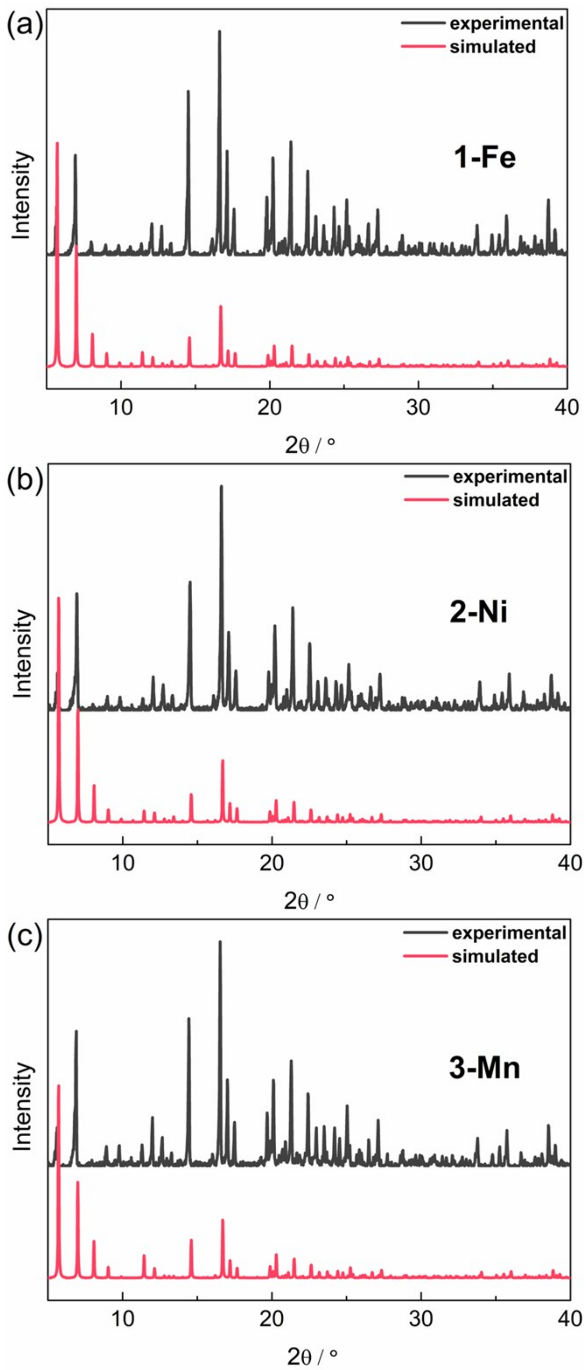

Fig. S2. X-ray powder diffraction data for compounds **1-3** at room temperature.

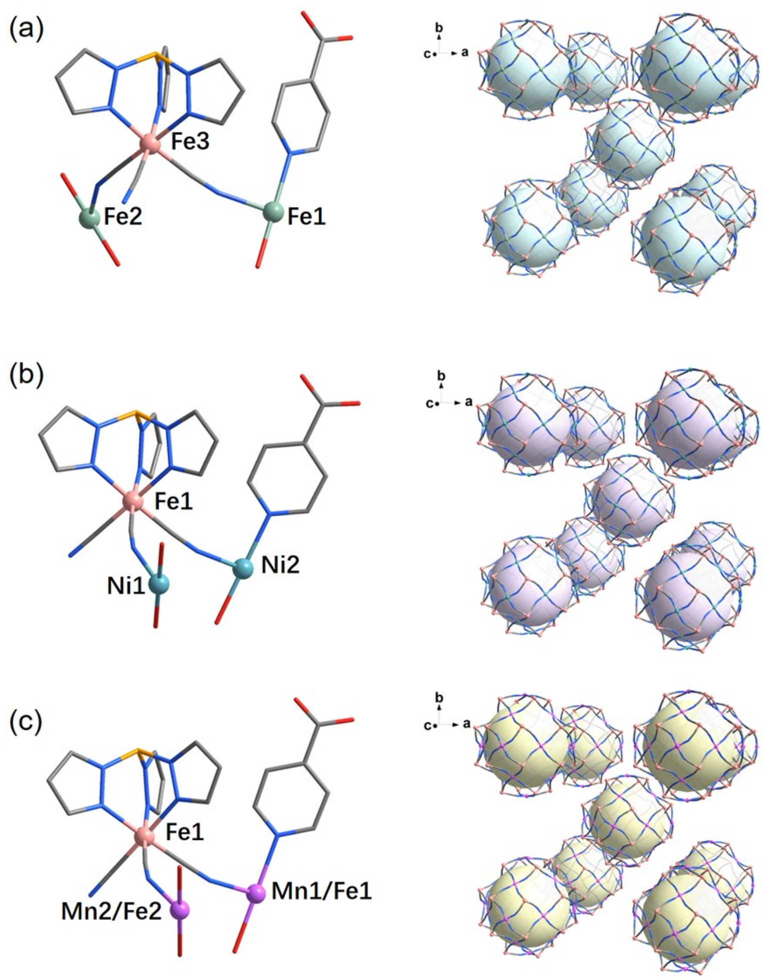

Fig. S3. (a) The asymmetric unit and crystal packing for cyanide-bridged framework of **1-Fe**. (b) The asymmetric unit and crystal packing for cyanide-bridged framework of **2-Ni**. (c) The asymmetric unit and crystal packing for cyanide-bridged framework of **3-Mn**. Color code: Fe from $[Fe(NC)_4(H_2O)_2]$ and $[Fe(NC)_4(L)(H_2O)]$, green; Ni from $[Ni(NC)_4(H_2O)_2]$ and $[Ni(NC)_4(L)(H_2O)]$, cyan; Mn from $[Mn(NC)_4(H_2O)_2]$ and $[Mn(NC)_4(L)(H_2O)]$, purple; Fe from $[Fe(Tp)(CN)_3]$, pink; N, blue; C, gray; B, yellow; O, red. Hydrogen atoms and solvents are omitted for clarity.

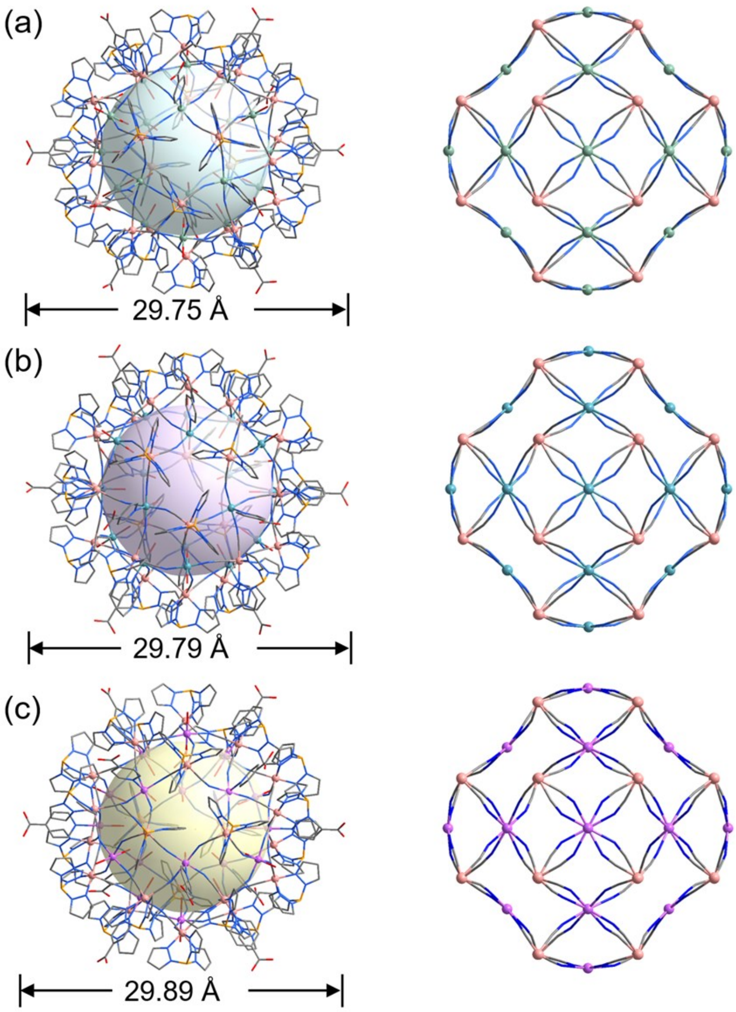

Fig. S4. A frame structure of a single {$Fe_{24}M_{18}$} nanocage and the skeleton structure with metal ions bridged by cyanide groups for **1-Fe** (a), **2-Ni** (b) and **3-Mn** (c).

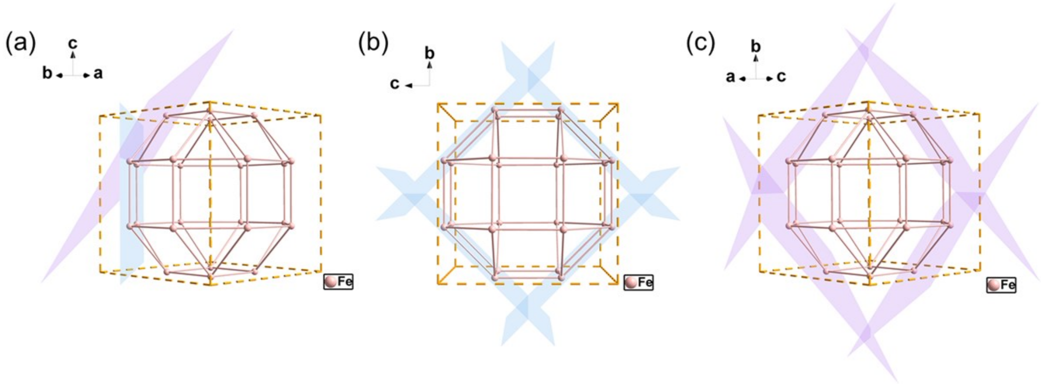

Fig. S5. Construction of the pseudo-rhombicuboctahedron through cut of the cubic (a), first cut all the edges of cubic (b) and then cut all angles of cubic (c).

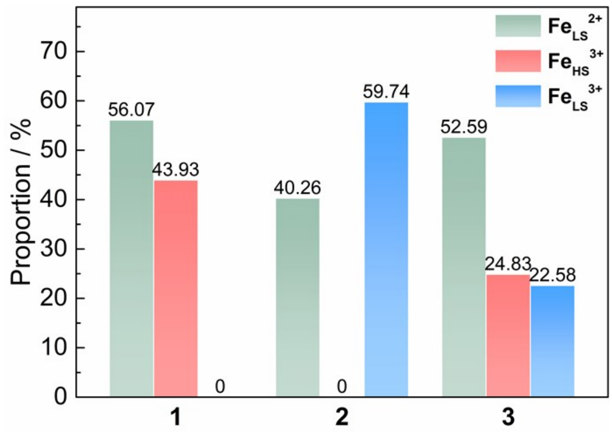

Fig. S6. Peak area ratio of different type of Fe species obtained from Mössbauer spectra.

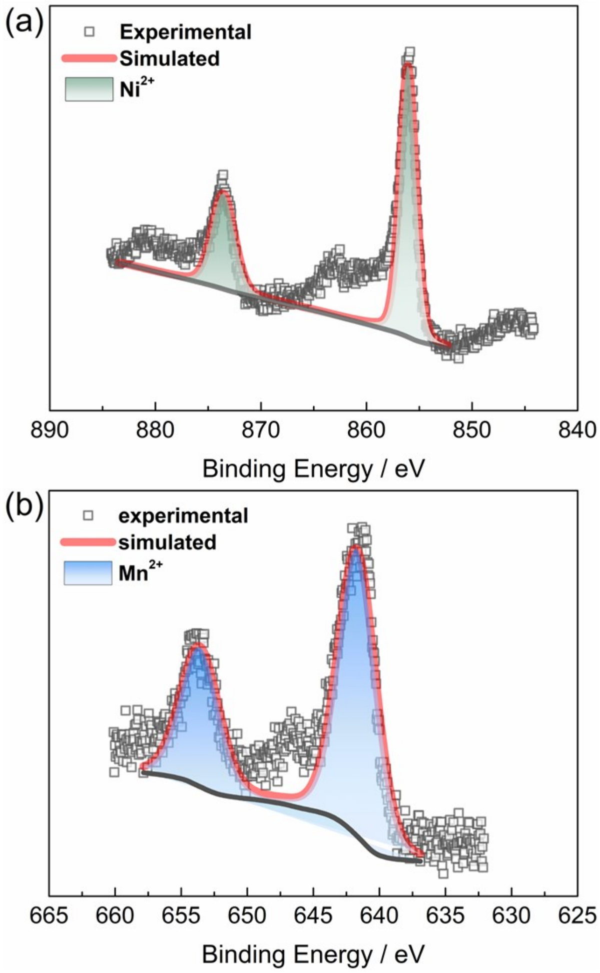

Fig. S7. (a) XPS spectra of Ni 2p for compound **2**, the binding energy around 856.1 eV and 873.6 eV can be attributed to Ni^{II}. (b) XPS spectra of Mn 2p for compound **3**, the binding energy around 641.8 eV and 653.5 eV can be attributed to Mn^{II}.

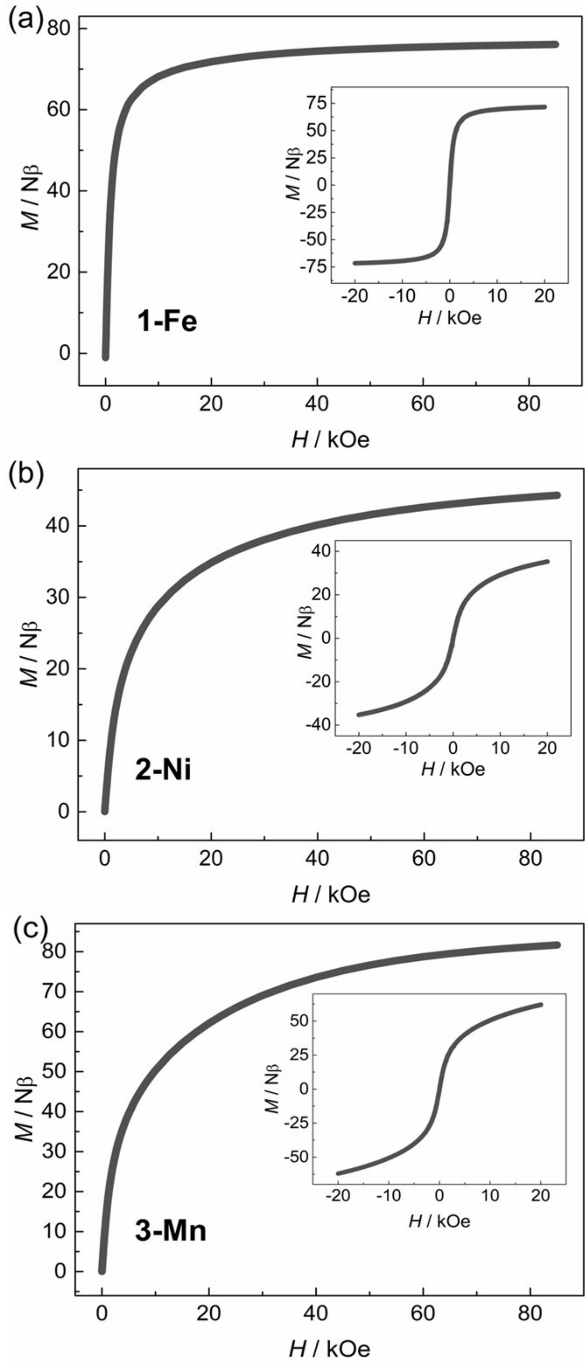

Fig. S8. Field-dependent of magnetic susceptibility for compounds **1-3** at 1.8 K. Inset: Field-dependent of magnetic susceptibility loop for compounds **1-3** at 1.8 K.

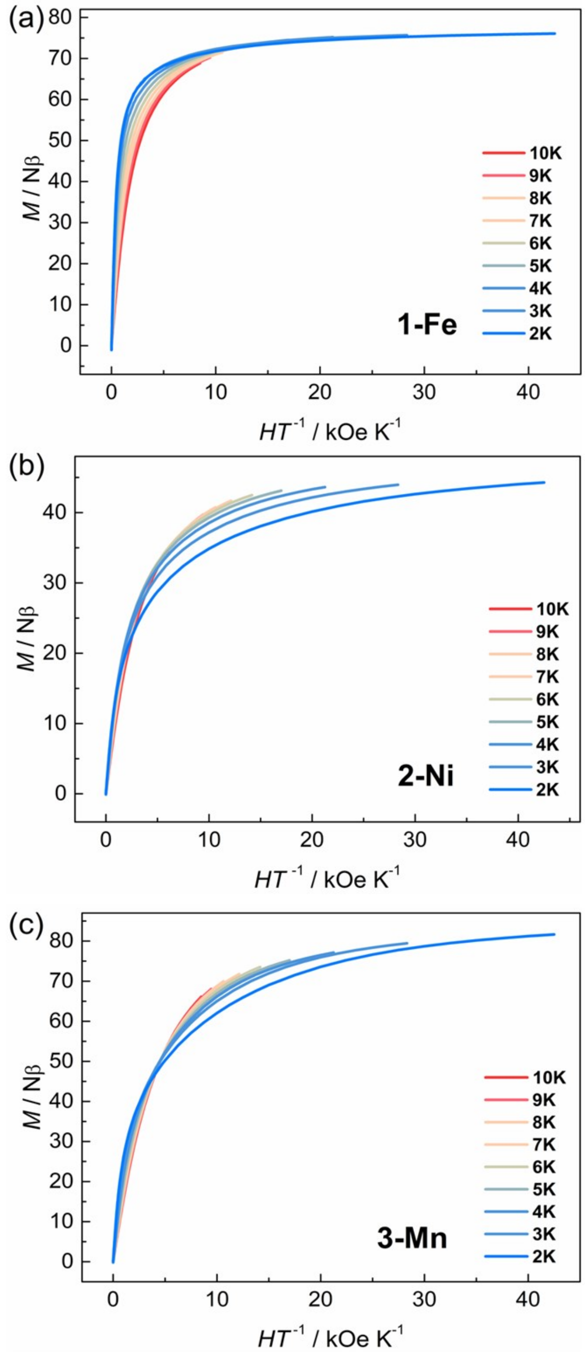

Fig. S9. Plot of magnetization (M/N_β) vs HT^{-1} in the range of 2-10 K for compounds **1-3**.